



THE UNIVERSITY *of* EDINBURGH

Edinburgh Research Explorer

Car-Parrinello and path integral molecular dynamics study of the hydrogen bond in the chloroacetic acid dimer system

Citation for published version:

Morrison, C 2007, 'Car-Parrinello and path integral molecular dynamics study of the hydrogen bond in the chloroacetic acid dimer system', *Journal of Chemical Physics*, vol. 127, no. 6, pp. 064304.
<https://doi.org/10.1063/1.2749251>

Digital Object Identifier (DOI):

[10.1063/1.2749251](https://doi.org/10.1063/1.2749251)

Link:

[Link to publication record in Edinburgh Research Explorer](#)

Document Version:

Publisher's PDF, also known as Version of record

Published In:

Journal of Chemical Physics

Publisher Rights Statement:

Copyright 2007 American Institute of Physics. This article may be downloaded for personal use only. Any other use requires prior permission of the author and the American Institute of Physics.

General rights

Copyright for the publications made accessible via the Edinburgh Research Explorer is retained by the author(s) and / or other copyright owners and it is a condition of accessing these publications that users recognise and abide by the legal requirements associated with these rights.

Take down policy

The University of Edinburgh has made every reasonable effort to ensure that Edinburgh Research Explorer content complies with UK legislation. If you believe that the public display of this file breaches copyright please contact openaccess@ed.ac.uk providing details, and we will remove access to the work immediately and investigate your claim.



Car-Parrinello and path integral molecular dynamics study of the hydrogen bond in the chloroacetic acid dimer system

Piotr Durlak, Carole A. Morrison, Derek S. Middlemiss, and Zdzislaw Latajka

Citation: *J. Chem. Phys.* **127**, 064304 (2007); doi: 10.1063/1.2749251

View online: <http://dx.doi.org/10.1063/1.2749251>

View Table of Contents: <http://jcp.aip.org/resource/1/JCPSA6/v127/i6>

Published by the **AIP Publishing LLC**.

Additional information on *J. Chem. Phys.*

Journal Homepage: <http://jcp.aip.org/>

Journal Information: http://jcp.aip.org/about/about_the_journal

Top downloads: http://jcp.aip.org/features/most_downloaded

Information for Authors: <http://jcp.aip.org/authors>

ADVERTISEMENT



Explore the **Most Cited**
Collection in Applied Physics

AIP
Publishing

Car-Parrinello and path integral molecular dynamics study of the hydrogen bond in the chloroacetic acid dimer system

Piotr Durlak

Faculty of Chemistry, University of Wrocław, 14 F. Joliot-Curie, 50-383 Wrocław, Poland

Carole A. Morrison^{a)}

School of Chemistry, and EaSTCHEM Research School, University of Edinburgh, The King's Buildings, West Mains Road, Edinburgh, EH9 3JJ, United Kingdom

Derek S. Middlemiss

Department of Chemistry and WESTCHEM Research School, University of Glasgow, University Avenue, Glasgow, G12 8QQ, United Kingdom

Zdzislaw Latajka

Faculty of Chemistry, University of Wrocław, 14 F. Joliot-Curie, 50-383 Wrocław, Poland

(Received 23 March 2007; accepted 22 May 2007; published online 9 August 2007)

We have studied the double proton transfer (DPT) reaction in the cyclic dimer of chloroacetic acid using both classical and path integral Car-Parrinello molecular dynamics. We also attempt to quantify the errors in the potential energy surface that arise from the use of a pure density functional. In the classical dynamics a clear reaction mechanism can be identified, where asynchronized DPT arises due to coupling between the O–H stretching oscillator and several low energy intermolecular vibrational modes. This mechanism is considerably altered when quantum tunneling is permitted in the simulation. The introduction of path integrals leads to considerable changes in the thermally averaged molecular geometry, leading to shorter and more centered hydrogen bond linkages.
© 2007 American Institute of Physics. [DOI: 10.1063/1.2749251]

I. INTRODUCTION

Fast proton transport (PT) between donor and acceptor atoms is of paramount importance in many aspects of chemistry and biology. Applications are diverse and include many technological developments such as hydrogen fuel cells, electrochromic displays, gas/humidity sensors, and electrochemical reactors.¹ Awareness of the fundamental properties of complex PT mechanisms is also central to our evolving understanding of biological processes. In nature all reactions that convert energy from one form into another are mediated by PT, which also serves as a vital route to achieve cell pH stabilization.²

The basic mechanism of PT is highly complex as it involves coupling between several different molecular vibrational modes, in addition to any other interactions which may take place within, e.g., a liquid or protein environment. The specific case of double proton transfer (DPT), to which this work is addressed, represents another layer of complexity. Recent applications of experimental and theoretical methods to model DPT systems have made considerable progress, and to a certain level of approximation the phenomenon is now understood. Experimental evidence is hard to obtain, as the observation of ultrafast vibrational dynamics requires the use of advanced methods based on multidimensional nonlinear coherent laser spectroscopies. There have been several recent studies on cyclic carboxylic acid dimers^{3–5} and other simple systems,^{6,7} which have given rise to the discovery that the

O–H stretching motions are coupled anharmonically to lower frequency vibrational modes, that are in turn responsible for modulating the length of the hydrogen bond. This basic structural mechanism establishes a continuum of potential energy surface (PES) shapes, from the double well at hydrogen bond lengths around 2.6 Å, to the single well around 2.4 Å. As a consequence the PT barrier height depends explicitly upon the heavy atom positions, and the transfer process cannot be understood within an adiabatic, or averaged thermal structure perspective. There have also been several theoretical reports based on cyclic formic acid dimers^{8–13} and other systems.^{13,14} In particular, Ushiyama and Takatsuka⁹ set out a clear reaction mechanism based on *ab initio* (Hartree-Fock) chemical dynamics and Miura *et al.*¹⁰ used Car-Parrinello molecular dynamics¹⁵ (CPMD) calculations to demonstrate the impact of quantum fluctuations [as represented within a path integral (PIMD) formalism^{16–18}] upon the transfer events.

From a theoretical perspective the accurate modeling of proton transport is a challenge for three main reasons. First, bond formation and breaking events are not described by conventional molecular mechanics force fields. Second, owing to the small mass of the hydrogen atom, quantum effects such as tunneling and zero-point energy contributions can radically alter the reaction landscape. Third, the proton transfer step is a rare event; put simply, if one were to perform standard molecular dynamics (MD) calculations, prohibitively long trajectories would need to be obtained in order to provide a reasonable sampling of transfer events.

There are several different computational approaches

^{a)}Electronic mail: c.morrison@ed.ac.uk

that can be taken. In an attempt to address all three issues raised above we have opted to study DPT in a simple model system to avoid compromise on the level of calculation that can be performed. Our system of choice is the gas phase cyclic dimer formed by chloroacetic acid, the rationale being that the chloroderivative is a stronger acid than the parent compound and is therefore likely to have a faster rate of DPT. As such, the reaction should occur spontaneously with a rate that is accessible by quantum mechanical MD calculations. We have adopted the same approach as Miura *et al.*, namely, a CPMD simulation,¹⁵ in which the positions of the atoms evolve according to the classical equations of motion, on the basis of forces obtained directly from the instantaneous electronic structure. This is then followed with a PIMD simulation,^{16–18} which explores the quantum behavior of both the nuclear and electronic degrees of freedom within the Born-Oppenheimer approximation. In essence it maps the problem of a quantum particle into one of a classical ring polymer model with beads that interact through temperature and mass-dependent spring forces. In practice, the representation of each atom in the system as group of N beads requires N electronic structure calculations, and therefore adds considerably to the computational expense. The one saving grace of the method is that the N calculations are (almost) entirely independent, and can therefore be successfully farmed out on a multiprocessor high performance computer.

While an *ab initio* MD simulation can be regarded as a current state-of-the-art technique, a problem arises in application to PT reactions. In these calculations, the full many-electron Hamiltonian is typically approximated within a density functional theory (DFT) approach,^{19,20} and the resulting Kohn-Sham orbitals expanded via a plane-wave basis set.²¹ Modeling the bond dissociation limit presents a particular difficulty for current exchange-correlation functionals, for they lack the nonlocal contributions essential for the accurate modeling of a bond stretched to its breaking point, resulting typically in an underestimation of PT barrier heights.^{22,23} Hybrid-DFT functionals, which include some component of the inherently nonlocal Hartree Fock (HF) exchange, tend to produce more realistic barrier heights. However, the use of such functionals requires diagonalization of the Fock matrix, which is prohibitively expensive in a plane wave representation. Although there are algorithms in development that promise to render HF theory with plane waves more tractable, they are not yet within the public domain, and so MD with hybrid functionals remains unavailable at the present time. A further problem which arises in simulations of PT is the neglect of zero-point contributions (ZPC) in classical dynamics, although the PIMD method can account for this effect at finite temperature. It is always important to be aware of the weaknesses in any modeling approach, and in this work we will attempt to quantify them.

In this paper we first present the results obtained from a series of geometry and transition state optimizations for the cyclic chloroacetic acid dimer using a localized basis set approach, where we add HF exchange in stepwise increments into the BLYP (Ref. 24) DFT functional in order to gauge the likely barrier height inaccuracies in our *ab initio* MD simulations. The effects of the ZPC upon the DPT reaction are

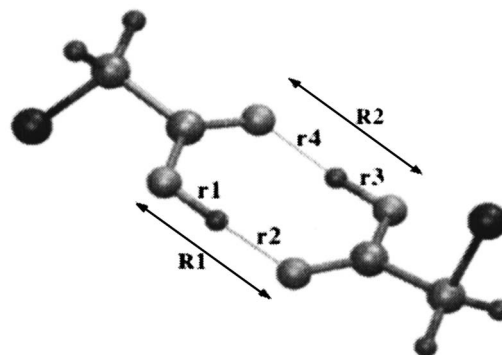


FIG. 1. Structure and atomic labeling for the chloroacetic acid dimer.

also assessed. The classical MD results are presented next, followed by a discussion of the impact on the DPT event of the quantum mechanical treatment of the nuclear motion obtained within PIMD. Finally we present results obtained for the deuterated bridge analogue, to discover the effects of isotopic substitution on the reaction mechanism.

II. COMPUTATIONAL DETAILS

A. Localized basis set modeling

A series of geometry optimizations and vibrational frequency calculations were performed to characterize the key stationary points on the PES of the chloroacetic acid dimer (see Fig. 1) using the GAUSSIAN03 simulation package.²⁵ In addition, in an attempt to quantify the shortcomings in a pure DFT functional approach (as employed in our subsequent MD calculations) we undertook a series of calculations employing hybrid functionals containing a variable mixture of the Becke88 (Ref. 24) and Fock exchange potentials with VWN (Ref. 26) and LYP (Ref. 24) correlation, as defined by the following form:

$$P_2 E_x^{\text{HF}} + P_1 (P_4 E_x^{\text{Slater}} + P_3 \Delta E_x^{\text{Becke}}) + P_6 E_c^{\text{VWN}} + P_5 \Delta E_c^{\text{LYP}}.$$

The standard B3LYP functional is obtained by setting parameters P_1 to P_6 to values of 1.0, 0.2, 0.72, 0.8, 0.81, and 1.0, respectively. In the current work we set P_3 to P_6 to 0.9, 1.0, 0.81, and 1.0, respectively, and varied P_2 from 0 (yielding pure DFT exchange, i.e., the BLYP functional) to 1 (pure Fock exchange, i.e., HF+LYP) in stepwise increments while maintaining the corresponding weight of DFT-based exchange, P_1 , at $1 - P_2$. Standard 6-311++G** basis sets were used for all atoms. The ground state was optimized in the C_1 point group with maximum (rms) force tolerances of 0.00045 (0.0003) a.u. and maximum (rms) displacement tolerances of 0.0018 (0.0012) a.u. The DPT transition state was obtained by optimizations of identical quality within the C_2 point group, which maintained centered hydrogen bond proton positions. Zero-point contributions to ground and transition state energies were obtained from harmonic frequency analysis, which also confirmed the saddle point character of the transition state.

TABLE I. Ground and transition state bond lengths (Å) and Cl–C–O(H) dihedral angles, ϕ (°), energy difference between structures lacking zero-point contribution, ΔE (kJ mol⁻¹ dimer⁻¹), and including ZPC, $\Delta E(\text{ZPC})$ (kJ mol⁻¹ dimer⁻¹) for varying fractional contents of Fock exchange, P_2 .

P_2	Ground state			Transition state			ΔE	$\Delta E(\text{ZPC})$
	O··O	O–H	ϕ	O··O	O–H	ϕ		
0.0	2.677	1.015	78.7	2.440	1.220	90.0	21.562	5.332
0.1	2.680	1.006	78.2	2.426	1.213	90.0	25.476	8.400
0.2	2.684	0.998	77.0	2.414	1.207	90.0	29.328	11.477
0.3	2.682	0.991	76.0	2.403	1.201	90.0	33.079	14.546
0.4	2.682	0.985	74.4	2.392	1.196	90.0	36.691	17.512
0.5	2.681	0.980	72.5	2.382	1.191	89.8	40.133	20.408
0.6	2.677	0.975	69.7	2.373	1.186	89.9	43.405	23.158
0.7	2.673	0.970	66.0	2.364	1.182	89.8	46.500	25.757
0.8	2.654	0.968	21.2	2.356	1.178	89.8	49.634	29.654
0.9	2.648	0.964	19.7	2.348	1.174	89.8	52.469	31.878
1.0	2.640	0.960	16.7	2.341	1.170	89.8	55.121	33.939

B. Molecular dynamics

Calculations have been carried out using the CPMD program,²⁷ with the initial molecular configuration for the chloroacetic acid dimer optimized by a pre-conditioned conjugate gradients algorithm. The dimer was located in a simple cubic box of dimension 11.0 Å. Molecular dynamics and path integral simulations (within the *nvt* ensemble) were carried out at 450 K with a time step of 3.0 a.u., coupled to Nosé-Hoover thermostat^{28,29} chains for each vibrational degree of freedom at a characteristic frequency of 3000 cm⁻¹. An electronic mass parameter of 400 a.u. was employed. Electronic exchange and correlation have been modeled using the gradient-corrected functional of Perdew, Burke, and Ernzerhof (PBE).³⁰ Core electrons were treated using the norm-conserving atomic pseudopotentials of Troullier and Martins,³¹ while valence electrons were represented in a plane-wave basis set truncated at an extended energy cutoff of 80 Ry. Two types of molecular dynamics simulation have been carried out. In the first the behavior of all atoms was treated classically (CPMD), whereas in the second the nuclei were treated as quantum particles (PIMD).³² Following the initial equilibrium period, data were accrued over trajectories spanning 400 000 steps for the Car-Parrinello dynamics on the parent model and 200 000 steps for the deuterated-bridge model and the path integral dynamics simulation. The path integral simulation used ten beads and the normal mode variable transformation. The trajectory data were processed using the script of Kohlmeier³³ to calculate the arithmetic average position (the centroid) of each set of polymer beads prior to visualization using the VMD program.³⁴

III. RESULTS AND DISCUSSION

A. Localized basis set modeling

In common with other members of the carboxylic acid family, the monomer units of chloroacetic acid readily form cyclic dimers linked by a double hydrogen bond (see Fig. 1). The two minima that exist on the PES are linked via a transition state structure with centered proton positions. The low-

est energy structure corresponds to that where the chlorine atoms reside on opposite sides of the hydrogen bridge, as depicted in Fig. 1; twisting the terminal groups to the *cis* conformation resulted in a transition state just 0.3 kJ mol⁻¹ higher in energy (taking the ZPC correction into account).

The effect of varying the Fock exchange content of the hybrid functional on the ground and transition state structures, and resulting barrier heights, is summarized in Table I. There are notable structural changes as the amount of Fock exchange (P_2) is increased. For the ground state structure the covalent bond O–H steadily shortens, reaching a reduction of 5.4% of the pure DFT value at $P_2=1.0$. The O··O hydrogen bond length at first increases slightly, then steadily decreases to end up 1.4% shorter under HF+LYP conditions. There is an abrupt decrease in the Cl–C–O(H) torsional angle at $P_2>0.7$, but a curve of the ground state energy versus P_2 is smooth across the whole range. The transition state structure appears to be less sensitive, showing monotonic variation in bond lengths and a torsional angle that varies slightly, but remains close to 90°.

Turning now to discuss energies, we observe that as P_2 increases the barrier height also steadily increases. This supports the findings of Sadhukhan *et al.*,²² who demonstrated that the B3LYP functional underestimated and the HF method overestimated the barrier height of their model PT reaction. The study by Poater *et al.*²³ suggests that a value of $P_2=0.5$ should give a close approximation to the true barrier height, based on calculations of model gas-phase chemical reactions. We conclude therefore that the implication for an *ab initio* MD study is that the use of a pure DFT functional is likely to lead to an underestimation of the reaction barrier height by a factor of approximately 2 (see Table I).

In addition to considering the deficiencies in the functional, it is also essential to consider the effect of neglecting the ZPC in an *ab initio* MD simulation. From Table I it is immediately apparent that this has a profound effect on the reaction barrier height. The large contribution arises from the fact that, at the transition point, it is the O–H stretching mode that becomes imaginary, and it is this mode which makes the largest contribution to the ZPC. Neglect of the ZPC therefore

results in an overestimation of the barrier height by a factor of about 2.

There are therefore two competing deficiencies in our *ab initio* classical MD simulations, which might be expected to partially cancel in a fortuitous manner. The pure DFT functional will underestimate the DPT barrier, but the neglect of the ZPC will work against this to our favor. Although these test calculations employed a different DFT functional (BLYP) to the one actually used in our MD calculations (PBE), a similar effect should hold for this functional. The net result is likely to be a barrier height of around $20 \text{ kJ mol}^{-1} \text{ dimer}^{-1}$ for the DPT reaction in the classical MD simulation. Finally, we have also considered the effect of full deuteration upon the ZPC; energy barriers are increased by a close-to-constant $6 \text{ kJ mol}^{-1} \text{ dimer}^{-1}$ across the range of P_2 values.

B. Classical dynamics

The necessary starting point for a molecular dynamics simulation is the optimized athermal geometry. This structure subsequently provides a useful reference point to assess the effects of thermal fluctuations on the molecular geometry. In particular, we observe that the average $\text{O}\cdots\text{O}$ distance expands by some 0.15 \AA at 450 K . Changes in the hydrogen bond internal parameters (as defined in Fig. 1) are presented in Fig. 2. From this it is evident that there are two distinct behaviors of the system: a rest period, where each proton remains closely associated with one oxygen atom and exhibits normal O–H vibrational behavior, and an active period, where both protons quickly transfer to the other well on the PES.³⁵ In the classical dynamics this process can proceed only by a thermal hopping mechanism, that is, the protons must pass over the top of the barrier. In total we observed the double proton transfer event occurring eight times during the 33 ps trajectory.

The eight DPT events therefore yield sixteen individual PT incidents that can be closely examined. The following chain of events observed for the first PT event (see Fig. 3) are apparently replicated throughout the data set and is consistent with a classical proton “hopping” mechanism.¹ The first indicator that a proton hopping event will occur is a contraction in the $\text{O}\cdots\text{O}$ distance to around $2.3\text{--}2.4 \text{ \AA}$. This change in geometry is commensurate with a drop in barrier height on the PES, facilitating the movement of the proton. In nearly all incidents, the proton hop event follows approximately 10 fs later. This time interval corresponds to a frequency of around 3000 cm^{-1} , which most probably correlates with the O–H vibration. The driver for the proton to return to its original site is then a second contraction of the $\text{O}\cdots\text{O}$ distance. The time scale from initiation of the hop to movement into the other well is around 15 fs, which finds agreement with previous studies of urea-phosphoric acid,³⁶ benzoylacetone,³⁷ and the PT events observed by Ushiyama and Takatsuka for the formic acid dimer.⁹

Dreyer *et al.* have investigated the complex line shape of the O–H stretching band in the gas phase cyclic dimer of acetic acid through a combined coherent femtosecond IR-pump-IR-probe spectroscopy and quantum mechanical mod-

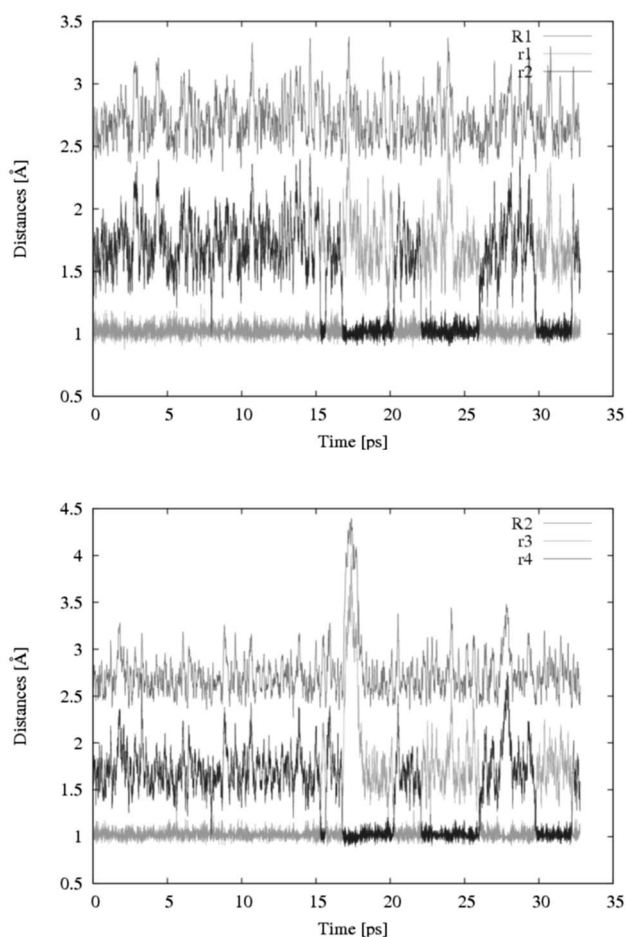


FIG. 2. Hydrogen bond distances as a function of time from the classical dynamics simulation.

eling study.^{3,4} In particular, this work identified two modes which couple strongly to $\nu\text{O–H}$, which are the hydrogen bond bending (δ_{dimer}) and stretching (ν_{dimer}) modes, at wave numbers of 145 and 170 cm^{-1} , respectively. Both of these low energy normal modes of vibration modulate the hydrogen bond distance strongly. For the choroderivative the harmonic vibrational frequency analysis using the BLYP functional predicts the same modes to appear at around 140 and 240 cm^{-1} , respectively. In an effort to determine whether these modes are implicated in our simulation, we have Fourier transformed the R1, R2 and r1, r3 distance versus time plots presented in Fig. 3. We observe common peaks in all the resulting plots at 140 and 245 cm^{-1} , indicating that the motions of the $\text{O}\cdots\text{O}$ and O–H bonds are correlated at these frequencies. It seems reasonable, therefore, to suggest that the basic mechanism for PT within the classical dynamics trajectories involves coupling between $\nu\text{O–H}$ and the low energy δ_{dimer} and ν_{dimer} intermolecular modes.

There are other issues pertaining to the double hydrogen bond linkage that need to be addressed, such as whether the two hydrogen atoms display synchronous or asynchronous behavior. During the rest periods, our data support an asynchronous behavior of the two bridging protons [i.e., as r1 increases r3 decreases, and vice versa; see Fig. 4(a)], which finds agreement with the formic acid dimer studies of Miura *et al.*¹⁰ and Ushiyama and Takatsuka.⁹ During the active pe-

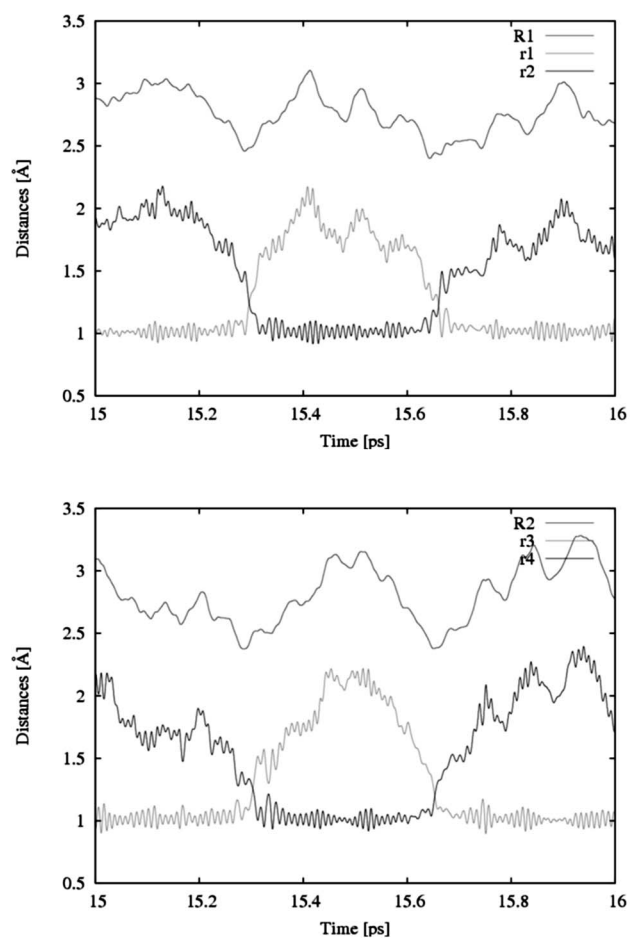


FIG. 3. First DPT event observed in the classical dynamics simulation.

roids Ushiyama and Takatsuka propose a two-step mechanism for DPT, that is, the two protons do not pass the mid-points of their respective hydrogen bonds at exactly the same time. We also observe this detail in our simulation and note a small time delay of just less than 10 fs (cf. the value of 8 fs found by Ushiyama and Takatsuka).

The complete mechanism for DPT proposed by Ushiyama and Takatsuka is that the first proton thermally hops to the other well without large deformation of the skeleton O–C–O bonds. There then arises a small time delay while the orders of the C–O and C=O bonds on both sides of the hydrogen bond linkage switch, and the second proton is then pulled across the hydrogen bond by the increased charge on the acceptor oxygen atom. Based on the fluctuations in structural parameters obtained directly from our CPMD simulation, we conclude that our data is entirely consistent with this mechanism. Ushiyama and Takatsuka also observed an interesting ordering in the proton hopping sequence for the formic acid dimer, namely, the second transferred proton becomes the first in the next DPT event, i.e., a hopping sequence of (H1,H2,H2,H1,H1,H2...) but offered no explanation for the effect. Our data are also largely consistent with this picture, with seven of the eight DPT events conforming to this pattern. Moreover, our data suggest that it is the ordering in the contraction of the two O···O distances that dictate which proton will be the first to transfer. This suggests that further coupling with other low energy modes must

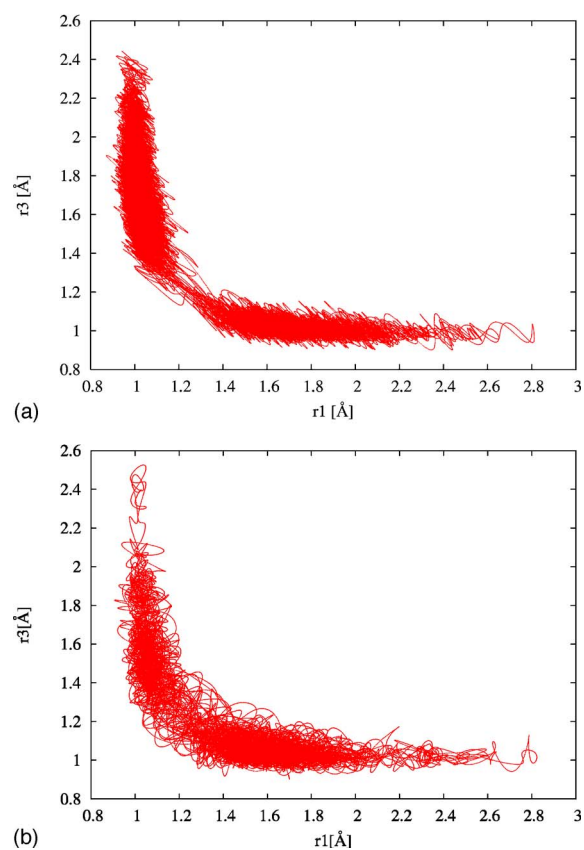


FIG. 4. Hydrogen bond distances r_1 vs r_3 by (a) classical dynamics and (b) path integral dynamics (based on the bead centroid positions).

be present, as the previously identified δ_{dimer} and ν_{dimer} modes cause the two O···O distances to contract in phase. Other studies have implicated interdimer rocking modes in the DPT mechanism that do induce asynchronous $r\text{O}\cdots\text{O}$ behavior⁴ and it is reasonable to postulate that this occurs in the current material too. We calculate the vibrational frequencies of two such intermolecular modes to appear at 165 cm^{-1} (rocking mode) and 202 cm^{-1} (bending mode) (BLYP/6-311++G*); on our Fourier transformed R1, R2, r1, and r3 CPMD distance plots we observe correlations at 160 and 195 cm^{-1} , which may be an indication that these modes are involved in the classical DPT mechanism.

Although the necessary condition for DPT would seem to be a contraction in the O···O distance, this alone is not sufficient to guarantee that the event will occur. Attempt frequencies in the low energy region of around 150–250 cm^{-1} corresponds to periods in the range of 0.15–0.20 ps, yielding about 200 opportunities for the DPT event within our data set. In order for just eight of those attempts to be successful the protons would have to climb a barrier height of around 14 $\text{kJ mol}^{-1} \text{dimer}^{-1}$, assuming an Arrhenius-type behavior of the reaction. We note in passing that this value is somewhat lower than that displayed in our test BLYP functional above (around 20 $\text{kJ mol}^{-1} \text{dimer}^{-1}$). However, we observe that the O···O distances in the MD trajectory frequently contract to a length below that observed in the localized basis set transition state structure, so the barrier overcome by the protons in the dynamical simulation may well be further reduced.

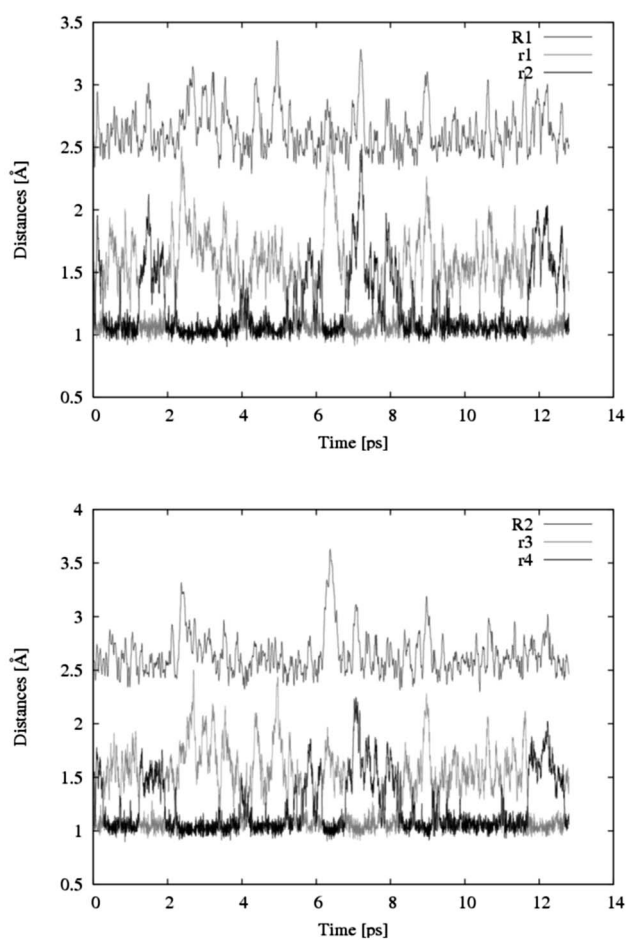


FIG. 5. Hydrogen bond distances as a function of time from the path integral dynamics simulation (based on the bead centroid positions).

C. Quantum dynamics

Following the classical dynamics, we obtained trajectories from path integral calculations in which each atom was represented as a 10-bead polymer. The beads interact through temperature and mass-dependent spring forces, and the model as a whole thus allows for a part of the quantum motion of the nuclei to be included. The results are presented in Fig. 5, where the changes in hydrogen bond internal parameters (based on the arithmetic average positions of the beads, i.e., the centroids) immediately suggest a much more dynamical and almost erratic system. This is also apparent in a histogram of O–H distances, which are plotted together for the classical and quantum dynamics for ease of comparison in Fig. 6. In addition to observing the active DPT periods, which occur much more frequently, there are now also a small number of transient single proton transfer (SPT) events, where a proton transfers from one oxygen to the other, but almost immediately moves back. Consequently, the rest periods are much less pronounced. Due to the considerable increase in computational resources required for this method, the total trajectory was sampled for just under half the total time of the classical simulation. The DPT phenomenon was observed about 20 times within this trajectory, indicating that the two proton bead centroids crossed the midpoints of their respective hydrogen bonds approximately

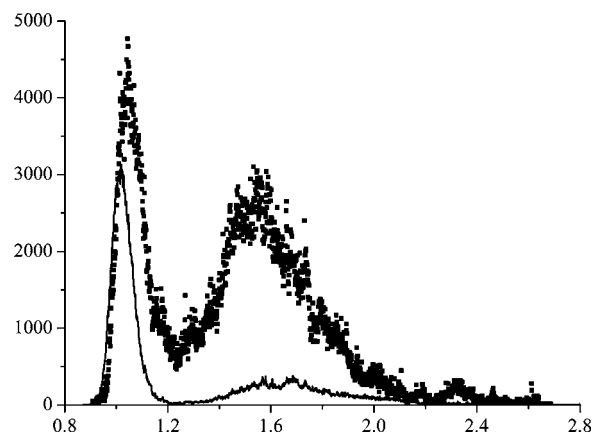


FIG. 6. Histograms of the O–H distances from classical (solid) and quantum dynamics (dotted, scaled by factor of 10).

five times more frequently than in the classical model. From this we conclude that the free energy barrier within quantum dynamics is significantly lower than in the classical dynamics, but it is difficult to relate the number of barrier crossings to a specific rate constant. Extensions to the PIMD method, which have gone some way toward the calculation of meaningful quantum reaction rate constants, are active areas of research and have been pursued by others. For example, Geva *et al.* have developed centroid molecular dynamics,³⁸ which is based on the hypothesis that quantum effects can be incorporated into the bead centroids which in turn follow classical-like dynamics. Craig and Manolopoulos have developed the ring polymer molecular dynamics^{39,40} method, which is a generalization of PIMD to calculate the approximate Kubo-transformed real-time correlation functions. The application of these methods to obtain a meaningful quantum rate constant is an obvious future direction of this work.

The conditions established in the classical simulation for DPT are seemingly relaxed in the quantum mechanical dynamics. While the DPT events do still occur following the shortening of R1 and R2, the contraction appears to be less pronounced, with nearly all incidences occurring across O···O distances of greater than 2.4 Å, indicating a tunneling mechanism. It is of great interest to note that there are significant differences in the heavy atom structure in the quantum dynamics. The average O···O distance (measured with respect to the centroid positions of the polymer beads) is considerably shorter and oscillates through a narrower range of values [2.64(18) Å PIMD vs 2.73(24) Å classical]. This compares favorably with the results of a gas electron diffraction study of the parent acetic acid dimer, which reported $r_{\text{O}\cdots\text{O}}$ at 2.680(10) Å.⁴¹ In addition, the O–H distance in the resting phase is longer by some 0.03 Å, compared with the classical result (see Fig. 6). It is clear, therefore, that the bridging hydrogen atoms spend more time in close proximity to the barrier. This in turn implies that the frequency $\nu_{\text{O-H}}$ of proton approaches to the barrier region, which manifests as the 10 fs delay for the first proton transfer in the classical trajectory, will be of reduced consequence in the quantum dynamics. This is supported by our data, where the delay was absent in nearly all DPT incidences. Indeed in a small number of cases the hydrogen atoms were observed to transfer before the O···O contraction.

The general asynchronous behavior of the two protons is maintained [see Fig. 4(b)], where a direct comparison with the classical results shows a greater spread in r_1 , r_3 (centroid) values. The increased occupancy at the transition state ($r_1=r_3$ =around 1.2 Å) is also apparent. It should be noted, however, that a comparison with the similar results reported by Miura *et al.* (based on a 20-polymer-bead model) shows that our values vary over a narrower range, which suggest that we may not have included a sufficient number of replicas to fully capture the quantum nature of this system. Further analysis of the PIMD data set reveals other differences in the DPT mechanism as compared with the classical model, the most pertinent being that in nearly all of the observed instances the hydrogen atoms are now synchronized at the actual point of DPT, which finds agreement with the PIMD study on the formic acid dimer by Miura.

The mechanism for DPT in quantum dynamics therefore seems to involve a considerable relaxation of the strict criteria extracted from the classical model. The shorter average O \cdots O distance and longer O–H distance means that the rest positions of the bridging hydrogen atoms are closer to the PES barrier. Proton transfer can occur over distances greater than 2.4 Å and the time delay attributed to the ν O–H approach frequency seems no longer a set requirement. At the actual point of DPT the heavy skeletal O–C–O and both hydrogen atoms all move simultaneously.

Finally, we comment on the rare and transient SPT events. Our data suggests that the reason for these failed attempts is linked to the absence of the appropriate switch in the C–O/C=O heavy atom geometry.

D. Deuterium-bridged analogue

For completeness, we also present a study of the cyclic chloroacetic acid dimer in which the bridging hydrogen atoms are substituted for deuterium. The deuterium tunneling rate is expected to be considerably lower than that observed for hydrogen, and so we conducted only a classical dynamics simulation in this case. In the data collection period (15 ps) double deuterium transfer (DDT) was observed six times, suggesting a system of slightly higher activity compared to the hydrogen-bridged dimer. However, the transfer events have occurred so infrequently that it is difficult to make reliable comments about the rate without resorting to repeating the dynamics runs or collecting data for significantly longer periods of time.

While the likelihood of tunneling is lower, other changes induced by isotopic substitution may be expected. The geometric isotope effect, whereby hydrogen bond distances expand upon deuteration, is essentially due to ZPC,⁴² and this would seem to argue for the necessity of including quantum effects in the dynamics. However, a recent review that examined the body of diffraction data published over many decades concluded that the expansion in O \cdots O distances (of the order 0–0.03 Å) was observed only in short to moderate hydrogen bonds of length between 2.4 and 2.65 Å.⁴³ The hydrogen bonds in this study are of length greater than 2.7 Å and are therefore unlikely to display a significant effect. In the simulation, the substitution of deuterium for hydrogen

resulted in virtually no change in the hydrogen bond parameters, with average O \cdots O distances of 2.74(22) and 2.73(24) Å for the hydrogen and deuterium-bridged models, respectively. The average O–H and O–D rest distances were identical, at 1.02(4) Å.

Some general comments on the reaction mechanism can be drawn from the six recorded DDT events. The contraction in the O \cdots O distance prior to deuterium transfer is less pronounced, with all events occurring over distances longer than 2.4 Å, i.e., some 0.05–0.1 Å longer than for DPT. As a consequence it is harder to identify the starting point of the reaction, and it is therefore difficult to identify whether the deuterium transfer occurs after a longer time delay which would be attributed to the lower ν O–D approach frequency. The time taken for deuterium to move from one side of the hydrogen bond to the other is of a similar magnitude for a proton (15 fs). Finally, the time delay between the two deuterium atoms passing the midpoints of their respective hydrogen bonds is less than for the hydrogen analogue; however, further work is required to verify this observation.

IV. CONCLUSIONS

We have studied the classical and quantum mechanical reaction mechanism for rare double proton transfer events in the cyclic chloroacetic acid dimer using *ab initio* molecular dynamics. While the methods used are recognized as state of the art they have important limitations, among the most notable of which are the absence of contributions from excited electronic states and the underestimation of reaction barrier heights arising from the use of functionals which omit important nonlocal exchange and correlation effects. Furthermore, the classical dynamics simulation neglects the vibrational zero-point contribution to the reaction energetics, but we estimate that this may act to largely counteract the error in barrier height.

Under classical conditions the DPT proceeds via a thermal hopping mechanism, facilitated by the ν O–H oscillator acting in concert with several low energy intermolecular vibrational modes that act to close the donor-acceptor distance, thereby reducing the barrier height. We identify the hydrogen bond bending, stretching, and rocking motions as the most important modes in this regard, and note that the latter causes the O \cdots O distances to contract in an alternate manner and thus dictates the sequence in which the protons transfer. Following the thermal hop of the first proton, there is a short time delay while the orders of the C–O and C=O bonds on both sides of the hydrogen bond linkage switch, which then permits the second proton to transfer. Substitution of deuterium for hydrogen results in no appreciable difference in the thermally averaged structures. Differences in the mechanism of the transfer reaction seem to exist within our data, with the transfer occurring at longer O \cdots O distances, and the two bridging atoms appearing to act in a more synchronized fashion.

Modeling the quantum behavior of the atoms by a 10-bead polymer model dramatically altered the reaction pathway and increased the number of DPT events by an order of 5. The criteria observed for DPT under classical conditions

are seemingly relaxed, with the two protons transferring in a synchronous fashion over donor-acceptor distances which are typically greater than 2.4 Å, and without the delay attributed to the approach frequency $\nu_{\text{O-H}}$. At the actual point of DPT, the heavy skeletal O-C-O and both hydrogen atoms all move simultaneously. There are also significant changes in the heavy atom geometry, leading to shorter and more centered hydrogen bond linkages that are more akin to the experimental structure. From a structural chemistry perspective this effect is very significant, as we have previously observed that classical *ab initio* molecular dynamics calculations report slightly longer, more asymmetric hydrogen bonds than measured experimentally.³⁶ Thus we note that the introduction of a path integral treatment, at even the modest levels reported here, can significantly improve upon the thermally averaged structure.

ACKNOWLEDGMENTS

The authors acknowledge the use of the University of Edinburgh's e-Server Blue Gene System, the support of EPCC, and the Academic Computer Center in Gdansk (TASK). The authors thank Professor Paul A. Madden for helpful discussions during the preparation of this manuscript. One of the authors (P.D.) acknowledges the support of the HPC-Europa programme, funded under the European Commission's Research Infrastructures activity of the Structuring the European Research Area programme, Contract No. RII3-CT-2003-506079. One of the authors (C.A.M.) also thanks the Royal Society for the award of a Royal Society Research Fellowship. Two of the authors (C.A.M. and D.S.M.) thank the EPSRC for funding under Grant No. GR/T21615.

¹K. D. Kreuer, *Chem. Mater.* **8**, 610 (1996).

²R. J. P. Williams, *Annu. Rev. Biophys. Biophys. Chem.* **17**, 71 (1988).

³J. Dreyer, *Int. J. Quantum Chem.* **104**, 782 (2005).

⁴K. Heyne, N. Huse, J. Dreyer, E. T. J. Nibbering, T. Elsaesser, and S. Mukamel, *J. Chem. Phys.* **121**, 902 (2004).

⁵K. Heyne, N. Huse, E. T. J. Nibbering, and T. Elsaesser, *Chem. Phys. Lett.* **369**, 591 (2003).

⁶J. Stenger, D. Madsen, J. Dreyer, E. T. J. Nibbering, P. Hamm, and T. Elsaesser, *J. Phys. Chem. A* **105**, 2929 (2001).

⁷A. Fernando-Ramos, Z. Smedarchina, and J. Rodrigues-Otero, *J. Chem. Phys.* **114**, 1567 (2001).

⁸N. Shida, P. F. Barbara, and J. Almlöf, *J. Chem. Phys.* **94**, 3633 (1991).

⁹H. Ushiyama and K. Takatsuka, *J. Chem. Phys.* **115**, 5903 (2001).

¹⁰S. Miura, M. E. Tuckerman, and M. L. Klein, *J. Chem. Phys.* **109**, 5290 (1998).

¹¹T. Loerting and K. R. Liedl, *J. Am. Chem. Soc.* **120**, 12595 (1998).

¹²Y. Kim, *J. Am. Chem. Soc.* **118**, 1522 (1996).

¹³K. Wolf, A. Simperler, and W. Mikenda, *Monatsh. Chem.* **130**, 1031 (1999).

¹⁴N. Sato and S. Iwata, *J. Chem. Phys.* **89**, 2932 (1988).

¹⁵R. Car and M. Parrinello, *Phys. Rev. Lett.* **55**, 2471 (1985).

¹⁶M. E. Tuckerman, D. Marx, M. L. Klein, and M. Parrinello, *J. Chem. Phys.* **104**, 5579 (1996).

¹⁷M. E. Tuckerman, B. J. Berne, G. J. Martyna, and M. L. Klein, *J. Chem. Phys.* **99**, 2796 (1993).

¹⁸D. Marx and M. Parrinello, *Z. Phys. B: Condens. Matter* **95**, 143 (1994); *J. Chem. Phys.* **104**, 4077 (1996).

¹⁹P. Hohenberg and W. Kohn, *Phys. Rev.* **136**, B864 (1964).

²⁰W. Kohn and L. J. Sham, *Phys. Rev.* **140**, A1133 (1965).

²¹M. C. Payne, M. P. Teter, D. C. Allan, T. A. Arias, and J. D. Joannopoulos, *Rev. Mod. Phys.* **64**, 1045 (1992).

²²S. Sadhukhan, D. Muñoz, C. Adamo, and G. E. Scuseria, *Chem. Phys. Lett.* **306**, 83 (1999).

²³J. Poater, M. Solà, M. Duran, and J. Robles, *Phys. Chem. Chem. Phys.* **4**, 722 (2002).

²⁴BLYP requests the Becke88 functional and the correlation functional of Lee, Yang and Parr. A. D. Becke, *Phys. Rev. A* **38**, 3098 (1988); C. Lee, W. Yang, and R. G. Parr, *Phys. Rev. B* **37**, 785 (1988).

²⁵M. J. Frisch, G. W. Trucks, H. B. Schlegel *et al.*, computer code GAUSSIAN 03, revision C.02, Gaussian, Inc., Wallingford, CT, 2004.

²⁶S. H. Vosko, L. Wilk, and M. Nusair, *Can. J. Phys.* **58**, 1200 (1980).

²⁷CPMD version 3.11.1, Copyright IBM Corp. 1990–2006, Copyright MPI für estkörperforschung Stuttgart 1997–2001.

²⁸S. Nosé, *J. Chem. Phys.* **81**, 511 (1984).

²⁹W. G. Hoover, *Phys. Rev. A* **31**, 1695 (1985).

³⁰J. P. Perdew, S. Burke, and M. Ernzerhof, *Phys. Rev. Lett.* **77**, 3865 (1996).

³¹N. Troullier and J. L. Martins, *Phys. Rev. B* **43**, 1993 (1991).

³²M. Parrinello and A. Rahman, *J. Chem. Phys.* **80**, 860 (1984).

³³traj2xyz.pl, ver.1.4, 2004/07/12-Axel Kohlmeyer.

³⁴W. Humphrey, A. Dalke, and K. Schulten, *J. Mol. Graphics* **14**, 33 (1996).

³⁵Note the spike in R2 on Fig. 3(b) at around 17 ps relates to a temporary breaking of this hydrogen bond due to intermolecular vibration of the dimer unit.

³⁶C. A. Morrison, M. M. Siddick, P. J. Camp, and C. C. Wilson, *J. Am. Chem. Soc.* **127**, 4042 (2005).

³⁷S. Pantano, F. Alver, and P. Carloni, *J. Mol. Struct.: THEOCHEM* **530**, 177 (2000).

³⁸E. Geva, Q. Shi, and G. A. Voth, *J. Chem. Phys.* **115**, 9209 (2001).

³⁹I. R. Craig and D. E. Manolopoulos, *J. Chem. Phys.* **122**, 084106 (2005).

⁴⁰I. R. Craig and D. E. Manolopoulos, *J. Chem. Phys.* **123**, 034102 (2005).

⁴¹J. L. Derissen, *J. Mol. Struct.* **7**, 67 (1971).

⁴²J. M. Robertson and A. R. Ubbelohde, *Proc. R. Soc. London, Ser. A* **170**, 222 (1939).

⁴³M. Ichikawa, *J. Mol. Struct.* **552**, 63 (2000).